

Nonlinear Analysis: Modelling and Control, Vol. 21, No. 4, 477–497
<http://dx.doi.org/10.15388/NA.2016.4.4>

ISSN 1392-5113

Stability and bifurcation analysis of Westwood+ TCP congestion control model in mobile cloud computing networks*

Hongyan Yu, Songtao Guo, Fei Wang

College of Electronic and Information Engineering, Southwest University
Chongqing 400715, China
stguo@swu.edu.cn

Received: August 9, 2014 / **Revised:** January 21, 2015 / **Published online:** March 14, 2016

Abstract. In this paper, we first build up a Westwood+ TCP congestion control model with communication delay in mobile cloud computing networks. We then study the dynamics of this model by analyzing the distribution ranges of eigenvalues of its characteristic equation. Taking communication delay as the bifurcation parameter, we derive the linear stability criteria depending on communication delay. Furthermore, we study the direction of Hopf bifurcation as well as the stability of periodic solution for the Westwood+ TCP congestion control model with communication delay. We find that the Hopf bifurcation occurs when the communication delay passes a sequence of critical values. The stability and direction of the Hopf bifurcation are determined by the normal form theory and the center manifold theorem. Finally, numerical simulation is done to verify the theoretical results.

Keywords: Hopf bifurcation, Westwood+ TCP, congestion control algorithm, stability, mobile cloud computing.

1 Introduction

Mobile cloud computing combines wireless mobile access service and wired cloud computing to improve the performance of mobile applications by offloading data processing from mobile devices to servers. However, running mobile applications in the mobile cloud computing networks requires both radio resources (e.g., wireless bandwidth) and computing resources (e.g., CPU, memory and storage). These resources need to be efficiently managed to maximize the utilization of the resources and thereby maximize the revenues of the mobile cloud service providers. With the rapid increase of mobile devices and applications, they compete for radio and computing resources being unaware of each other

*This research was supported by the National Natural Science Foundation of China (61373179, 61402381), Fundamental Research Funds for the Central Universities (XDJK2013A018, XDJK2013C094), the Doctoral Research Funds of Southwest University (SWU113020), Educational Science Research Programming of Hubei Province (B20132508) and Natural Science Key Foundation of Chongqing (cstc2015jcyjBX0094).

and the current state of resources. In this setting, congestion arises when the demand for bandwidth exceeds the available link capacity. This will lead to performance degradation in the network as packet losses increase and link utilization decreases. As a result, network congestion control has become a main concern in mobile cloud computing networks.

In order to deal with congestion, Jacobson [16] proposed a classical transmission control protocol (TCP), which is based on a sliding window mechanism and employs an additive increase multiplicative decrease (AIMD) algorithm in per Round Trip Time (RTT). The whole congestion control system is a combination of the end-to-end TCP congestion control mechanism at sources and the active queue management (AQM) mechanism at routers. The aim of AQM mechanism is to estimate congestion level at each router before congestion occurs and provide feedback information to senders by either dropping or marking packets. So far, many AQM algorithms, such as Random Early Detection (RED) [7] and Random Early Marking (REM) [1], have been proposed.

Such a classical TCP model is appropriate for enabling end-to-end reliable communication over the Internet as well as avoiding network congestion and collapse. In the next few years, the classical TCP model is a standard for ensuring end-to-end reliable delivery of packets and is used by a large variety of applications. However, the classical TCP is originally designed for wired low error rate networks, it assumes that all packet losses are caused by network congestion. Unlike wired networks, in wireless networks, many of packet losses are due to noisy and fading radio channel, which are often misinterpreted as a symptom of congestion by the classical TCP scheme and thus cause an unnecessary window reduction. Therefore, AIMD algorithms can ensure that network capacity is not exceeded, but they cannot ensure fair sharing of capacity [18]. Moreover, they provide a low throughput in the presence of losses not due to congestion, such as in the case of radio links [2].

Recently, in order to improve the capability of classical TCP to track the available bandwidth, Westwood TCP proposed by Mascolo et al. [23] substitutes the multiplicative decrease with an adaptive decrease phase, that is, it follows an additive increase adaptive decrease (AIADD) congestion control algorithm and filters the stream of returning acknowledgements (ACKs). However, Westwood TCP heavily depends on bandwidth estimation, and the original bandwidth estimation algorithm proposed in [23] does not work properly in the presence of ACK compression [9]. In order to overcome such drawbacks, a new bandwidth estimate algorithm, Westwood+ TCP, was proposed in [8]. The key idea of Westwood+ TCP is to exploit the stream of return acknowledgment packets to estimate the available bandwidth by the AIADD paradigm, which is extremely effective for throughput improvements in mixed wired and wireless networks required by mobile cloud computing. It motivates us to analyze the nonlinear dynamic behavior of the Westwood+ TCP in mobile cloud computing networks.

In general, a congestion control system may be considered as a complex nonlinear feedback system with delay by reducing mathematical model of congestion control system to a nonlinear delay differential equation (NDDE). Therefore, in recent years, nonlinear dynamic behavior of congestion control system in communication network has attracted much attention from researchers. In [24], Massoulié et al. studied the stability of distributed congestion control with heterogeneous feedback delays. Furthermore, the

fairness, delays and stability of end-to-end congestion control were analyzed in [17, 19]. Liu et al. proposed an exponential-RED algorithm and analyzed its stability for low- and high-speed TCP protocols [22]. However, how does TCP/AQM system evolves when the congestion control system loses its stability? This field also begins to draw much attention from researchers [4, 5, 6, 10, 11, 12, 13, 14, 20, 21, 25, 26, 27, 28, 29, 32, 33]. In [27], Raina et al. found that if the local stability of TCP with drop tail is just lost, the corresponding nonlinear system undergoes a supercritical Hopf bifurcation. In [29], the delay induced Hopf bifurcation was studied in a simplified network congestion control model. In [4, 5], Ding et al. analyzed Hopf bifurcation in a fluid flow model and a dual model of Internet congestion control algorithm. Moreover, we studied stability and Hopf bifurcation analysis in a novel congestion control model with communication delay and heterogeneous delays in [10, 11, 14] and analyzed Hopf bifurcation in an exponential RED algorithm with communication delay and heterogeneous delays in [12, 13]. Xu et al. studied bifurcation analysis and control in exponential RED algorithm in [32]. More recently, Dong et al. analyzed dynamics of a congestion control model in a wireless access network [6]. Xiao et al. studied bifurcation control of internet congestion control model via state feedback [30, 31].

Nevertheless, to the best of our knowledge, there are few papers to discuss the bifurcation of Westwood+ TCP congestion control algorithm, especially, with the communication delay consisting of wired communication delay and wireless delay. We consider communication delay as an important factor that cannot be ignored, because it plays an imperative role in improving network stability, fair bandwidth allocation and resource utilization of high speed wired and wireless networks. Although Grieco et al. analyzed the dynamics of Westwood+ TCP congestion control algorithm and provided the locally asymptotically stable conditions of equilibrium points in [9], they did not consider the effect of communication delay on Westwood+ TCP model. Motivated by the above discussions, we aim in this paper to study the stability and Hopf bifurcation of Westwood+ TCP congestion control algorithm in mobile cloud computing networks and provide the conditions of Hopf bifurcation occurring.

In this paper, we will first build up a Westwood+ TCP model with communication delay by analyzing its AIADD process, which is one of our main contributions. We then move our attention to study nonlinear dynamic behavior of the proposed Westwood+ TCP with communication delay, including its stability and Hopf bifurcation. During analyzing dynamic behavior, we take the communication delay as the bifurcation parameter. The reason is that complex dynamics of Westwood+ TCP congestion control system are often related to wired and wireless communication delay. The presence of delay plays an important role in the stability and performance of Westwood+ TCP congestion control system. If the delay is beyond the range to guarantee a stable system, it will lead to instability and degradation of system performance.

The rest of this paper is organized as follows. In Section 2, we introduce Westwood+ TCP congestion control model. In Section 3, we derive linear stability criteria of the Westwood+ TCP model and the existence of Hopf bifurcation by analyzing the distribution ranges of the corresponding characteristic equations of the linearized equation of the proposed Westwood+ TCP model with communication delay. Section 4 is devoted

to the direction and stability analysis of Hopf bifurcation based on the normal theory and center manifold approach. Numerical simulations are given in Section 5. Finally, Section 6 concludes this paper.

2 Westwood+ TCP congestion control model with communication delay

In this section, we will model the dynamics of the expected transmission rate of an AIADD controlled Westwood+ TCP flow as a function of the segment loss probability, the bandwidth estimate and the connection round trip time (RTT). We let p be the drop probability of a segment, τ_R denotes the mean round trip time, T_0 be a time constant, τ represents communication delay, $r(t)$ denotes the rate at which source transmits data at time t , \hat{B} specifies the bandwidth estimation from the impulse response of a first-order low-pass filter, and $\tau_{R_{\min}}$ stands for the minimum round trip time, i.e., slow start threshold to a value of bandwidth estimation (BWE) times.

In a Westwood+ TCP flow model [9], the congestion window is updated upon ACK reception. The receiver transmits one ACK packet once receiving one data. Each time the sender receives an ACK packet, it increases the congestion window W by $1/W$. Otherwise, once a segment is lost, the congestion window is set equal to $\hat{B} \times \tau_{R_{\min}}$. Accordingly, the change in W is $\hat{B} \times \tau_{R_{\min}} - W$. Thus, the variation of the congestion window W is a discrete random variable with the following probability function:

$$p(\Delta W) = \begin{cases} 1 - p & \text{when } \Delta W = 1/W, \\ p & \text{when } \Delta W = \hat{B} \times \tau_{R_{\min}} - W. \end{cases}$$

We then obtain the expected increment of congestion window W per update step as follows:

$$E(\Delta W) = \frac{1 - p}{W} + (\hat{B} \times \tau_{R_{\min}} - W)p.$$

In mobile cloud computing networks, the communication delay including wired communication delay and wireless delay exists widely due to the long-distance transmission of wired network, the link unreliability and channel fading of wireless networks. By considering the effect of communication delay τ on the congestion window, it is not difficult to obtain that the time between update steps is $\tau_R/W(t - \tau)$, i.e., $\Delta t = \tau_R/W(t - \tau)$. Thus, the expected change in the congestion window W per unit time is approximately given by

$$\frac{dW}{dt} = \frac{W(t - \tau)}{\tau_R} \left[\frac{1 - p}{W(t)} + p(\hat{B}(t) \times \tau_{R_{\min}} - W(t)) \right]. \quad (1)$$

In a bandwidth estimate model of Westwood+ TCP, we consider Westwood+ employs a first order low pass filter with time constant T_0 . To take into account the loss probability, we consider that the low-pass filter receives the rate $[1 - p(r(t))]r(t)$ of ACK packets. Therefore, the bandwidth estimate is the convolution of $[1 - p(r(t))]r(t)$ and $h(t)$, where

$h(t) = e^{-t/\tau_R}/\tau_R$ is the impulse response of a first-order low-pass filter:

$$\begin{aligned} \widehat{B}(t) &= \{[1 - p(r(t))]r(t)\} \times h(t) \\ &= \int_0^t [1 - p(r(\theta))]r(\theta)h(t - \theta) d\theta. \end{aligned} \tag{2}$$

Note that $p(r(t))$ is a function of the sending rate $r(t)$. In order to simplify the calculation, we suppose that $p(r(t)) = p$ is a constant. And by considering the effect of communication delay τ on the bandwidth estimate, (2) can be rewritten as follows:

$$\frac{d\widehat{B}}{dt} = -\frac{\widehat{B}(t - \tau)}{T_0} + \frac{1 - p}{T_0}r(t - \tau). \tag{3}$$

By combining (1) and (3), Westwood+ TCP congestion control model with communication delay can be given by

$$\begin{aligned} \frac{dW}{dt} &= \frac{W(t - \tau)}{\tau_R} \left[\frac{1 - p}{W(t)} + p(\widehat{B}(t) \times \tau_{R_{\min}} - W(t)) \right], \\ \frac{d\widehat{B}}{dt} &= -\frac{\widehat{B}(t - \tau)}{T_0} + \frac{1 - p}{T_0}r(t - \tau). \end{aligned} \tag{4}$$

3 Local stability and Hopf bifurcation analysis

In this section, we will analyze local stability and Hopf bifurcation of Westwood+ TCP congestion control model with communication delay. Substituting for $W(t) = \tau_R \times r(t)$, model (4) can be described by

$$\begin{aligned} \frac{dr}{dt} &= r(t - \tau) \left[\frac{1 - p}{\tau_R^2 r(t)} + p \left(\widehat{B}(t) \frac{\tau_{R_{\min}}}{\tau_R} - r(t) \right) \right], \\ \frac{d\widehat{B}}{dt} &= -\frac{\widehat{B}(t - \tau)}{T_0} + \frac{1 - p}{T_0}r(t - \tau). \end{aligned} \tag{5}$$

Throughout this paper, we assume $\tau, \tau_{R_{\min}}, \tau_R \geq 0$ and p are constants.

Let (r^*, B^*) be the non-zero equilibrium point of system (5), then we can obtain

$$r^* = \frac{\sqrt{(1 - p)/p}}{\sqrt{\tau_R[\tau_R - (1 - p)\tau_{R_{\min}}]}}, \quad B^* = (1 - p)r^*. \tag{6}$$

Let $x(t) = r(t) - r^*$ and $y(t) = \widehat{B}(t) - B^*$. Linearizing system (5) around the equilibrium point, by using (6), we can obtain

$$\begin{aligned} \frac{dx}{dt} &= ax(t) + by(t), \\ \frac{dy}{dt} &= cx(t - \tau) + dy(t - \tau), \end{aligned} \tag{7}$$

where $a = r^*p[(1 - p)\tau_{R_{\min}}/\tau_R - 2]$, $b = r^*p\tau_{R_{\min}}\tau_R$, $c = (1 - p)/T_0$, $d = -1/T_0$. Then the characteristic equation of equation (7) can be given by

$$D(\lambda, \tau) = \begin{bmatrix} \lambda - a & -b \\ -ce^{-\lambda\tau} & \lambda - de^{-\lambda\tau} \end{bmatrix} \\ = \lambda^2 - (a + de^{-\lambda\tau})\lambda + (ad - bc)e^{-\lambda\tau} = 0. \tag{8}$$

It is well known that the trivial solution of the nonlinear DDE (5) is locally asymptotically stable if all roots of the characteristic equation (8) satisfy $\text{Re}(\lambda) < 0$ (refer to [15]). In the following, we will study the existence of Hopf bifurcation of equation (5). Then we can obtain the following lemmas.

Lemma 1. Consider

$$D(\lambda, \tau) = \lambda^2 - a\lambda + [-d\lambda + (ad - bc)]e^{-\lambda\tau}. \tag{9}$$

If $\tau = 0$, then all zeros of $D(\lambda, \tau)$ have negative real parts.

Proof. When $\tau = 0$, we have

$$D(\lambda, 0) = \lambda^2 - (a + d)\lambda + (ad - bc).$$

Since $r^* > 0$, $0 < p < 1$, $0 < \tau_{R_{\min}} < \tau_R$, $T_0 > 0$, then $0 < 1 - p < 1$, $0 < \tau_{R_{\min}}/\tau_R < 1$. It is clear that $a = r^*p[(1 - p)\tau_{R_{\min}}/\tau_R - 2] < 0$. Furthermore, we have

$$a + d = r^*p \left[(1 - p)\frac{\tau_{R_{\min}}}{\tau_R} - 2 \right] + \left(-\frac{1}{T_0} \right) < 0.$$

Next, we prove that $ad - bc > 0$, which can be given by

$$ad - bc = r^*p \left[(1 - p)\frac{\tau_{R_{\min}}}{\tau_R} - 2 \right] \left(-\frac{1}{T_0} \right) - r^*p\frac{\tau_{R_{\min}}}{\tau_R} \left(\frac{1 - p}{T_0} \right) \\ = \frac{2r^*p[\tau_R - \tau_{R_{\min}}(1 - p)]}{\tau_R T_0}.$$

By equation (7), we know $\tau_R - \tau_{R_{\min}}(1 - p) > 0$. Then we have $ad - bc > 0$. Therefore, it is not difficult to obtain $\Delta = (a + d)^2 - 4(ad - bc) = (a - d)^2 + 4bc > 0$. We can obtain that all zeros of $D(\lambda, 0)$ have negative real parts. This completes the proof. \square

Lemma 2. When $\tau = \tau_0$, equation (8) has a simple pair of purely imaginary roots $\pm i\omega_0$, where

$$\omega_0 = \sqrt{\frac{(d^2 - a^2) + \sqrt{(d^2 - a^2)^2 + 4(ad - bc)^2}}{2}} \tag{10}$$

and

$$\tau_0 = \frac{1}{\omega_0} \left\{ \pi + \arctan \left[\frac{\omega_0^2 d + a(ad - bc)}{bc\omega_0} \right] \right\}. \tag{11}$$

Proof. We know that $i\omega_0, \omega_0 > 0$, is a root of equation (8) if and only if $i\omega_0$ satisfies

$$-\omega_0^2 - ai\omega_0 + [-di\omega_0 + (ad - bc)]e^{-i\omega_0\tau} = 0.$$

Equating the real and imaginary parts of both sides, we get

$$\begin{aligned} (ad - bc) \cos(\omega_0\tau) - d\omega_0 \sin(\omega_0\tau) &= \omega_0^2, \\ d\omega_0 \cos(\omega_0\tau) + (ad - bc) \sin(\omega_0\tau) &= -a\omega_0. \end{aligned} \tag{12}$$

It follows from (12) that

$$\omega_0^4 + (a^2 - d^2)\omega_0^2 - (ad - bc)^2 = 0. \tag{13}$$

It is clear that equation (13) has a unique positive root ω_0^2 .

Therefore, we have

$$\omega_0 = \sqrt{\frac{(d^2 - a^2) + \sqrt{(d^2 - a^2)^2 + 4(ad - bc)^2}}{2}},$$

and from equation (12) we also have

$$\sin \omega_0\tau = \frac{-\omega_0^3 d - a\omega_0(ad - bc)}{\omega_0^2 d^2 + (ad - bc)^2}, \quad \cos \omega_0\tau = \frac{-bc\omega_0^2}{\omega_0^2 d^2 + (ad - bc)^2}.$$

Then it follows that

$$\tau_0 = \frac{1}{\omega_0} \left\{ \pi + \arctan \left[\frac{\omega_0^2 d + a(ad - bc)}{bc\omega_0} \right] \right\}.$$

This completes the proof. □

Next we show that $\lambda = \pm i\omega_0$ are simple roots of equation (8) when $\tau = \tau_0$.

Differentiating the function

$$D(\lambda, \tau) = \lambda^2 - a\lambda + [-d\lambda + (ad - bc)]e^{-\lambda\tau}$$

with respect to λ , we can get

$$\frac{dD(\lambda, \tau)}{d\lambda} = 2\lambda - a - de^{-\lambda\tau} - \tau[-d\lambda + (ad - bc)]e^{-\lambda\tau}. \tag{14}$$

Substituting $\lambda = i\omega_0$ into equation (14), we can obtain

$$\frac{dD(i\omega_0, \tau)}{d\lambda} = [-a - \tau\omega_0^2 - d \cos \omega_0\tau] + [2\omega_0 - a\tau\omega_0 + d \sin \omega_0\tau]i \neq 0 \tag{15}$$

when $a < d$. Similarly, we can get

$$\frac{dD(-i\omega_0, \tau_0)}{d\lambda} \neq 0. \tag{16}$$

Hence, $\lambda = \pm i\omega_0$ are simple roots of equation (8) when $\tau = \tau_0$. Furthermore, according to our previous work [11], we have the following lemmas.

Lemma 3. When $\tau < \tau_0$, all the roots of (8) have strictly negative real parts.

Lemma 4. When $\tau = \tau_0$, except for the pair of purely imaginary roots $\pm i\omega_0$, all other roots of equation (8) have strict negative real parts.

Lemma 5. Let $\lambda(\tau) = \alpha(\tau) + i\omega(\tau)$ is the root of equation (8) satisfying $\alpha(\tau_0) = 0$, $\omega(\tau_0) = \omega_0$. The following transversally condition holds:

$$\left. \frac{d\text{Re}(\lambda(\tau))}{d\tau} \right|_{\tau=\tau_0} > 0. \tag{17}$$

Proof. By equation (8), with respect to τ and applying the implicit function theorem, we get

$$\frac{d\lambda(\tau)}{d\tau} = \frac{-\lambda[-d\lambda + (ad - bc)]e^{-\lambda\tau}}{2\lambda - a + [\tau(d\lambda - (ad - bc)) - d]e^{-\lambda\tau}},$$

then

$$\left(\frac{d\lambda(\tau)}{d\tau} \right)^{-1} = \frac{(2\lambda - a)e^{\lambda\tau} + \tau[d\lambda - (ad - bc)] - d}{-\lambda[d\lambda - (ad - bc)]}.$$

Since $\lambda(\tau_0) = i\omega_0$, hence, by equation (12), we can get

$$\begin{aligned} & \left(\frac{d\text{Re} \lambda(\tau)}{d\tau} \right)^{-1} \Big|_{\tau=\tau_0} \\ &= \frac{(-ad + 2bc)\omega_0 \cos \omega_0\tau + [2d\omega_0^2 + a(ad - bc)] \sin \omega_0\tau + d^2\omega_0}{-\omega_0[d^2\omega_0^2 + (ad - bc)^2]} \\ &= \frac{a[d\omega_0 \cos \omega_0\tau + (ad - bc) \sin \omega_0\tau] + 2\omega_0[d\omega_0 \sin \omega_0\tau - (ad - bc) \cos \omega_0\tau] + d^2\omega_0}{-\omega_0[d^2\omega_0^2 + (ad - bc)^2]} \\ &= \frac{2\omega_0^2 - (d^2 - a^2)}{d^2\omega_0^2 + (ad - bc)^2}. \end{aligned} \tag{18}$$

Since $2\omega_0^2 > (d^2 - a^2)$, then we have

$$\left(\frac{d\text{Re} \lambda(\tau)}{d\tau} \right)^{-1} \Big|_{\tau=\tau_0} > 0.$$

This completes the proof. □

Lemma 6. When $\tau > \tau_0$, equation (8) has at least one root with strictly positive real parts.

Proof. From Lemmas 4 and 5, by use of the lemma in [3], we can see that if $\tau > \tau_0$, equation (8) has at least one root with strictly positive real parts. □

Based on Lemmas 1–6, we can obtain the following theorem about local stability and hopf bifurcation of system (5) by applying Hopf bifurcation theory for delay differential equation [15].

Theorem 1. For system (5), the following results hold:

- (i) When $\tau < \tau_0$, the equilibrium point of system (5) is locally asymptotically stable.
- (ii) When $\tau > \tau_0$, the equilibrium point of system (5) is unstable.
- (iii) When $\tau = \tau_0$, system (5) occurs a Hopf bifurcation.

4 Direction and stability of Hopf bifurcation

In the previous section, we have obtained the condition for existence of Hopf bifurcation in congestion control system of Westwood+ TCP with communication delay at $\tau = \tau_0$. In this section, we shall study the direction of Hopf bifurcation, i.e., make it clear whether the bifurcating branch of periodic solution exists locally for $\tau > \tau_0$ or $\tau < \tau_0$, and stability of bifurcation period solution of system (5) at $\tau = \tau_0$ by employing the normal form method and center manifold theorem introduced by Hassard et al. in [15]. More precisely, we will compute the reduced system on the center manifold with the pair of conjugate complex, purely imaginary solutions of the characteristic equation (5). By this reduction, we can determine the Hopf bifurcation direction, i.e., to answer the question of whether the bifurcation branch of periodic solution exists locally for supercritical bifurcation or subcritical bifurcation.

The Taylor expansion of equation (5) about the equilibrium point is

$$\begin{aligned} \frac{dx}{dt} &= ax(t) + by(t) + a_{13}x^2(t) + a_{14}x(t - \tau)x(t) + a_{15}x(t - \tau)y(t), \\ \frac{dy}{dt} &= cx(t - \tau) + dy(t - \tau), \end{aligned} \tag{19}$$

where $a = r^*p[(1 - p)\tau_{R_{\min}}/\tau_R - 2]$, $b = r^*p\tau_{R_{\min}}/\tau_R$, $a_{13} = (1 - p)/(\tau_R^2r^{*2})$, $a_{14} = (p - 1)/(\tau_R^2r^{*2}) - p$, $a_{15} = p\tau_{R_{\min}}/\tau_R$, $c = (1 - p)/T_0$, $d = -1/T_0$.

Let $\tau = \tau_0 + \mu$, $u(t) = (x(t), y(t))^T$ and $u_t(\theta) = u(t + \theta)$ for $\theta \in [-\tau, 0]$. Then $\mu = 0$ is the Hopf bifurcation value for equation (5). Denote $C^k[-\tau, 0] = \{\varphi | \varphi : [-\tau, 0] \rightarrow R^2\}$. φ has k th-order continuous derivation. We can rewrite equation (19) as

$$\frac{du}{dt} = L_\mu u + F(u_t, \mu) \tag{20}$$

with

$$L_\mu \varphi = B_1 \varphi(0) + B_2 \varphi(-\tau) \tag{21}$$

and

$$F(\varphi, \mu) = \begin{pmatrix} a_{13}\varphi_1^2(0) + a_{14}\varphi_1(-\tau_0)\varphi_1(0) + a_{15}\varphi_1(-\tau_0)\varphi_2(0) \\ 0 \end{pmatrix}, \tag{22}$$

where $B_1 = \begin{pmatrix} a & b \\ 0 & 0 \end{pmatrix}$ and $B_2 = \begin{pmatrix} 0 & 0 \\ c & d \end{pmatrix}$.

Then L_μ is one parameter family of bounded linear operator in $C[-\tau, 0]$. By Reisz representation theorem, there exists a 2×2 matrix whose components are bounded variation functions

$$\eta(\cdot, \mu) : [-\tau, 0] \rightarrow R^{2 \times 2}$$

for $\varphi \in C[-\tau, 0]$ such that

$$L_\mu \varphi = \int_{-\tau}^0 d\eta(\theta, \mu) \varphi(\theta). \quad (23)$$

In fact, we can choose

$$\eta(\theta, \mu) = B_1 \delta(\theta) + B_2 \delta(\theta + \tau),$$

where $\delta(\theta)$ is Dirac delta function. Next, for $\varphi \in C[-\tau, 0]$, we define

$$A(\mu) \varphi = \begin{cases} d\varphi/d\theta, & \theta \in [-\tau, 0), \\ \int_{-\tau}^0 d\eta(\theta, \mu) \varphi(\theta) = L_\mu \varphi, & \theta = 0, \end{cases} \quad (24)$$

and

$$R(\mu) \varphi = \begin{cases} 0, & \theta \in [-\tau, 0), \\ F(\varphi, \mu), & \theta = 0. \end{cases} \quad (25)$$

Since $du_t/d\theta = du_t/dt$, (20) can be rewritten as

$$\frac{du_t}{dt} = A(\mu)u_t + R(\mu)u_t, \quad (26)$$

which is an equation of the form we desired. For $\theta \in [-\tau, 0)$, equation (26) is just the trivial equation $du_t/d\theta = du_t/dt$; for $\theta = 0$, it is (20).

For $\psi \in C[-\tau, 0]$, the adjoint operator A^* of A is defined as

$$A^* \psi = \begin{cases} -d\psi(s)/ds, & s \in (0, \tau], \\ \int_{-\tau}^0 d\eta^T(t, 0) \psi(-t), & s = 0. \end{cases} \quad (27)$$

For $\psi \in C[-\tau, 0]$ and $\varphi \in C[-\tau, 0]$, we define a bilinear form

$$\langle \psi, \varphi \rangle = \bar{\psi}^T(0) \varphi(0) - \int_{\theta=-\tau}^0 \int_{\xi=0}^{\theta} \bar{\psi}^T(\xi - \theta) [d\eta(\theta)] \varphi(\xi) d\xi, \quad (28)$$

where $\eta(\theta) = \eta(\theta, 0)$.

From the above analysis we know that $\pm i\omega_0$ are eigenvalues of $A(0)$. Let $q(\theta)$ be eigenvector of $A(0)$ corresponding to $i\omega_0$, then we have

$$A(0)q(\theta) = i\omega q(\theta).$$

Since $\pm i\omega_0$ are eigenvalues of $A(0)$ and other eigenvalues have strictly negative real parts, $\mp i\omega_0$ are the eigenvalues of $A^*(0)$. Then we have the following lemma.

Lemma 7. Let $q(\theta) = Ve^{i\omega_0\theta}$ be eigenvector of A associated with $i\omega_0$, and $q^*(\theta) = DV^*e^{i\omega_0\theta}$ be eigenvector of A^* associated with $-i\omega_0$. Then

$$\langle q^*, q \rangle = 1, \quad \langle q^*, \bar{q} \rangle = 0, \tag{29}$$

where

$$\begin{aligned} V &= (1, \rho_1)^T, & V^* &= (\rho_2, 1)^T; \\ \rho_1 &= \frac{i\omega_0\tau_R - r^*p[(1-p)\tau_{R_{\min}} - 2\tau_R]}{r^*p\tau_{R_{\min}}}, \\ \rho_2 &= \frac{\tau_R(p-1)e^{i\omega_0\tau_0}}{T_0r^*p[(1-p)\tau_{R_{\min}} - 2\tau_R] + i\omega_0T_0\tau_R}; \\ \bar{D} &= [\bar{V}^{*T}V + \tau_0e^{-i\omega_0\tau_0}\bar{V}^{*T}B_2V]^{-1}. \end{aligned}$$

Proof. Since $q(\theta)$ is eigenvector of A corresponding to $i\omega_0$, then we have

$$Aq(\theta) = i\omega_0q(\theta). \tag{30}$$

From (24) we can rewrite (30) as

$$\begin{aligned} \frac{dq(\theta)}{d\theta} &= i\omega_0q(\theta), \quad \theta \in [-\tau, 0), \\ L(0)q(0) &= i\omega_0q(0), \quad \theta = 0. \end{aligned} \tag{31}$$

Therefore, we can obtain

$$q(\theta) = Ve^{i\omega_0\theta}, \quad \theta \in [-\tau, 0], \tag{32}$$

where $V = (v_1, v_2)^T \in C^2$ is a constant vector. Based on (21) and (31), we have

$$[B_1 - i\omega_0I + B_2e^{-i\omega_0\tau_0}]V = 0,$$

where I is identity matrix. So, we can choose

$$V = \begin{pmatrix} v_1 \\ v_2 \end{pmatrix} = \begin{pmatrix} 1 \\ \frac{i\omega_0\tau_R - r^*p[(1-p)\tau_{R_{\min}} - 2\tau_R]}{r^*p\tau_{R_{\min}}} \end{pmatrix} = \begin{pmatrix} 1 \\ \rho_1 \end{pmatrix}. \tag{33}$$

From (27) we can get

$$A^*\psi = \int_{-\tau}^0 d\eta^T(t, 0)\psi(-t) = B_1^T\psi(0) + B_2^T\psi(\tau). \tag{34}$$

Let

$$q^*(\theta) = DV^*e^{i\omega_0\theta}, \quad \theta \in [0, \tau],$$

where $D = (d_1, d_2)^T, V^* = (v_1^*, v_2^*) \in C^2$ are constant vectors.

Similar to the proof of (30)–(33), we can obtain

$$V^* = \begin{pmatrix} v_1^* \\ v_2^* \end{pmatrix} = \begin{pmatrix} \frac{\tau_R(p-1)e^{i\omega_0\tau_0}}{T_0 r^* p[(1-p)\tau_{R\min} - 2\tau_R] + i\omega_0 T_0 \tau_R} \\ 1 \end{pmatrix} = \begin{pmatrix} \rho_2 \\ 1 \end{pmatrix}.$$

Now, we can calculate $\langle q^*, q \rangle$ as follows:

$$\begin{aligned} \langle q^*, q \rangle &= \overline{q^*}^T(0)q(0) - \int_{-\tau_0}^0 \int_{\xi=0}^{\theta} \overline{q^*}^T(\xi - \theta) [d\eta(\theta)] q(\xi) d\xi \\ &= \overline{D} \left[\overline{V^*}^T V - \int_{-\tau_0}^0 \int_{\xi=0}^{\theta} \overline{V^*}^T e^{-i\omega_0(\xi-\theta)} [d\eta(\theta)] V e^{i\omega_0\xi} d\xi \right] \\ &= \overline{D} \left[\overline{V^*}^T V - \int_{-\tau_0}^0 \int_{\xi=0}^{\theta} \overline{V^*}^T [d\eta(\theta)] \theta e^{i\omega_0\theta} V \right] \\ &= \overline{D} [\overline{V^*}^T V + \tau_0 e^{-i\omega_0\tau_0} \overline{V^*}^T B_2 V]. \end{aligned}$$

Thus, when $\overline{D} = [\overline{V^*}^T V + \tau_0 e^{-i\omega_0\tau_0} \overline{V^*}^T B_2 V]^{-1}$, we can get $\langle q^*, q \rangle = 1$.

On the other hand, since $\langle \psi, A\varphi \rangle = \langle A^*\psi, \varphi \rangle$, we have

$$-i\omega_0 \langle q^*, \bar{q} \rangle = \langle q^*, A\bar{q} \rangle = \langle A^*q^*, \bar{q} \rangle = \langle -i\omega_0 q^*, \bar{q} \rangle = i\omega_0 \langle q^*, \bar{q} \rangle.$$

Therefore, $\langle q^*, \bar{q} \rangle = 0$. This completes the proof. \square

In the remainder of this section, by using the same notion as in Hassard et al. [15], we first compute the coordinates to describe the center manifold center C_0 at $\mu = 0$, which is locally invariant, attracting two dimensional manifolds in C_0 . Let u_t be a solution of equation (19) when $\mu = 0$.

Define

$$\begin{aligned} z(t) &= \langle q^*, u_t \rangle, \\ W(t, \theta) &= u_t - zq - \bar{z}\bar{q} = u_t - 2\operatorname{Re}\{z(t)q(\theta)\}. \end{aligned} \quad (35)$$

On the center manifold C_0 , we have

$$W(t, \theta) = (z(t), \bar{z}(t), \theta),$$

where

$$W(z, \bar{z}, \theta) = W_{20}(\theta) \frac{z^2}{2} + W_{11}(\theta) z\bar{z} + W_{02} \frac{\bar{z}^2}{2} + \dots, \quad (36)$$

z and \bar{z} are local coordinates of center manifold C_0 in the direction of q^* and \bar{q}^* . Note that W is real if u_t is real. We only consider real solutions. From (36) we get

$$\begin{aligned} \langle q^*, W \rangle &= \langle q^*, u_t - zq - \bar{z}\bar{q} \rangle \\ &= \langle q^*, u_t \rangle - z(t) \langle q^*, q \rangle - \bar{z}(t) \langle q^*, \bar{q} \rangle = 0. \end{aligned}$$

For a solution $u_t \in C_0$ of (26), from (24) to (27), since $\mu = 0$, we have

$$\begin{aligned} \frac{dz(t)}{dt} &= \left\langle q^*, \frac{du_t}{dt} \right\rangle = \langle q^*, A(0)u_t + R(0)u_t \rangle \\ &= \langle A^* q^*, u_t \rangle + \overline{q^*}^T(0)F(u_t, 0) \\ &= i\omega_0 z(t) + \overline{q^*}^T(0)f_0(z, \bar{z}). \end{aligned}$$

We rewrite in abbreviates form as

$$\frac{dz(t)}{dt} = i\omega_0 z(t) + g(z, \bar{z}), \tag{37}$$

where

$$\begin{aligned} g(z, \bar{z}) &= \overline{q^*}^T(0)f_0(z, \bar{z}) \\ &= \overline{q^*}^T(0)F(W(z, \bar{z}, \theta) + 2 \operatorname{Re}\{z(t)q(t)\}, 0) \\ &= g_{20} \frac{z^2}{2} + g_{11} z\bar{z} + g_{02} \frac{\bar{z}^2}{2} + g_{21} \frac{z^2\bar{z}}{2} + \dots \end{aligned} \tag{38}$$

By (26) and (38), we have

$$\begin{aligned} \dot{W} &= \dot{u}_t - \dot{z}q - \dot{\bar{z}}\bar{q} \\ &= Au_t + Ru_t - i\omega_0 zq - \overline{q^*}^T(0)f_0(z, \bar{z})q + i\omega_0 \bar{z}\bar{q} - q^{*T}(0)\overline{f_0(z, \bar{z})\bar{q}} \\ &= Au_t + Ru_t - Azq - A\bar{z}\bar{q} - 2\operatorname{Re}\{\overline{q^*}^T(0)f_0(z, \bar{z})q\} \\ &= AW + Ru_t - 2 \operatorname{Re}\{\overline{q^*}^T(0)f_0(z, \bar{z})q\} \\ &= \begin{cases} AW - 2 \operatorname{Re}\{\overline{q^*}^T(0)f_0(z, \bar{z})q\}, & \theta \in [-\tau, 0), \\ AW - 2 \operatorname{Re}\{\overline{q^*}^T(0)f_0(z, \bar{z})q\} + f_0(z, \bar{z}), & \theta = 0. \end{cases} \end{aligned}$$

It can be rewritten as

$$\dot{W} = AW + H(z, \bar{z}, \theta), \tag{39}$$

where

$$H(z, \bar{z}, \theta) = H_{20}(\theta) \frac{z^2}{2} + H_{11}(\theta) z\bar{z} + H_{02} \frac{\bar{z}^2}{2} + \dots \tag{40}$$

On the other hand, on C_0 ,

$$\dot{W} = W_z \dot{z} + W_{\bar{z}} \dot{\bar{z}}. \tag{41}$$

Substituting (35) and (37) into (41) and comparing the coefficients of the above equation with those of equation (39), we get

$$\begin{aligned} H_{20}(\theta) &= -(A - i2\omega_0)W_{20}(\theta), \\ H_{11}(\theta) &= -AW_{11}(\theta), \\ H_{02}(\theta) &= -(A + i2\omega_0)W_{02}(\theta). \end{aligned} \tag{42}$$

Since $u_t = u(t + \theta) = W(z, \bar{z}, \theta) + zq + \bar{z}\bar{q}$, we have

$$u_t = \begin{pmatrix} x(t + \theta) \\ y(t + \theta) \end{pmatrix} = \begin{pmatrix} W^{(1)}(z, \bar{z}, \theta) \\ W^{(2)}(z, \bar{z}, \theta) \end{pmatrix} + z \begin{pmatrix} 1 \\ \rho_1 \end{pmatrix} e^{i\omega_0\theta} + \bar{z} \begin{pmatrix} 1 \\ \bar{\rho}_1 \end{pmatrix} e^{-i\omega_0\theta}.$$

Therefore, we can obtain

$$\begin{aligned} x(t + \theta) &= W^{(1)}(z, \bar{z}, \theta) + ze^{i\omega_0\theta} + \bar{z}e^{-i\omega_0\theta} \\ &= ze^{i\omega_0\theta} + \bar{z}e^{-i\omega_0\theta} + W_{20}^{(1)} \frac{z^2}{2} + W_{11}^{(1)} z\bar{z} + W_{02}^{(1)} \frac{\bar{z}^2}{2} + \dots \end{aligned}$$

and

$$\begin{aligned} y(t + \theta) &= W^{(2)}(z, \bar{z}, \theta) + z\rho_1 e^{i\omega_0\theta} + \bar{z}\bar{\rho}_1 e^{-i\omega_0\theta} \\ &= z\rho_1 e^{i\omega_0\theta} + \bar{z}\bar{\rho}_1 e^{-i\omega_0\theta} + W_{20}^{(2)} \frac{z^2}{2} + W_{11}^{(2)} z\bar{z} + W_{02}^{(2)} \frac{\bar{z}^2}{2} + \dots \end{aligned}$$

It is clear that

$$\begin{aligned} \varphi_1(0) &= z + \bar{z} + W_{20}^{(1)}(0) \frac{z^2}{2} + W_{11}^{(1)}(0) z\bar{z} + W_{02}^{(1)}(0) \frac{\bar{z}^2}{2} + \dots, \\ \varphi_1(-\tau_0) &= ze^{-i\omega_0\tau_0} + \bar{z}e^{i\omega_0\tau_0} + W_{20}^{(1)}(-\tau_0) \frac{z^2}{2} + W_{11}^{(1)}(-\tau_0) z\bar{z} + W_{02}^{(1)}(-\tau_0) \frac{\bar{z}^2}{2} + \dots, \\ \varphi_2(0) &= z\rho_1 + \bar{z}\bar{\rho}_1 + W_{20}^{(2)}(0) \frac{z^2}{2} + W_{11}^{(2)}(0) z\bar{z} + W_{02}^{(2)}(0) \frac{\bar{z}^2}{2} + \dots, \\ \varphi_1^2(0) &= z^2 + 2z\bar{z} + \bar{z}^2 + [2W_{11}^{(1)}(0) + W_{20}^{(1)}(0)] z^2\bar{z} + \dots, \\ \varphi_1(-\tau_0)\varphi_1(0) &= e^{-i\omega_0\tau_0} z^2 + (e^{i\omega_0\tau_0} + e^{-i\omega_0\tau_0}) z\bar{z} + e^{i\omega_0\tau_0} \bar{z}^2 \\ &\quad + \left[W_{11}^{(1)}(-\tau_0) + \frac{W_{20}^{(1)}(-\tau_0)}{2} + \frac{W_{20}^{(1)}(0)}{2} e^{i\omega_0\tau_0} + W_{11}^{(1)}(0) e^{-i\omega_0\tau_0} \right] z^2\bar{z} + \dots, \\ \varphi_1(-\tau_0)\varphi_2(0) &= \rho_1 e^{-i\omega_0\tau_0} z^2 + (\rho_1 e^{i\omega_0\tau_0} + \bar{\rho}_1 e^{-i\omega_0\tau_0}) z\bar{z} + \bar{\rho}_1 e^{i\omega_0\tau_0} \bar{z}^2 \\ &\quad + \left[W_{11}^{(2)}(0) e^{-i\omega_0\tau_0} + \frac{W_{20}^{(2)}(0)}{2} e^{i\omega_0\tau_0} + \frac{W_{20}^{(2)}(-\tau_0)}{2} \bar{\rho}_1 + W_{11}^{(2)}(-\tau_0) \rho_1 \right] z^2\bar{z} + \dots \end{aligned}$$

It follows that

$$\begin{aligned} f_0(z, \bar{z}) &= \begin{pmatrix} a_{13}\varphi_1^2(0) + a_{14}\varphi_1(-\tau_0)\varphi_1(0) + a_{15}\varphi_1(-\tau_0)\varphi_2(0) \\ 0 \end{pmatrix} \\ &= \begin{pmatrix} K_1 z^2 + K_2 z\bar{z} + K_3 \bar{z}^2 + K_4 z^2\bar{z} \\ 0 \end{pmatrix}, \end{aligned}$$

where

$$\begin{aligned}
 K_1 &= a_{13} + a_{14}e^{-i\omega_0\tau_0} + a_{15}\rho_1e^{-i\omega_0\tau_0}, \\
 K_2 &= 2a_{13} + a_{14}(e^{i\omega_0\tau_0} + e^{-i\omega_0\tau_0}) + a_{15}(\rho_1e^{i\omega_0\tau_0} + \bar{\rho}_1e^{-i\omega_0\tau_0}), \\
 K_3 &= a_{13} + a_{14}e^{i\omega_0\tau_0} + a_{15}\bar{\rho}_1e^{i\omega_0\tau_0}, \\
 K_4 &= a_{13}[2W_{11}^{(1)}(0) + W_{20}^{(1)}(0)] \\
 &\quad + a_{14}\left[W_{11}^{(1)}(-\tau_0) + \frac{W_{20}^{(1)}(-\tau_0)}{2} + \frac{W_{20}^{(1)}(0)}{2}e^{i\omega_0\tau_0} + W_{11}^{(1)}(0)e^{-i\omega_0\tau_0}\right] \\
 &\quad + a_{15}\left[W_{11}^{(2)}(0)e^{-i\omega_0\tau_0} + \frac{W_{20}^{(2)}(0)}{2}e^{i\omega_0\tau_0} + \frac{W_{11}^{(1)}(-\tau_0)}{2}\bar{\rho}_1 + W_{11}^{(1)}(-\tau_0)\rho_1\right].
 \end{aligned}$$

Since $\bar{q}^*(0) = \bar{D}(\bar{\rho}_2, 1)^T$, we have

$$\begin{aligned}
 g(z, \bar{z}) &= \bar{q}^{*T}(0)f_0(z, \bar{z}) = \bar{D}(\bar{\rho}_2, 1)f_0(z, \bar{z}) \\
 &= \bar{D}(\bar{\rho}_2, 1) \begin{pmatrix} K_1z^2 + K_2z\bar{z} + K_3\bar{z}^2 + K_4z^2\bar{z} \\ 0 \end{pmatrix} \\
 &= \bar{D}[K_1\bar{\rho}_2z^2 + K_2\bar{\rho}_2z\bar{z} + K_3\bar{\rho}_2\bar{z}^2 + K_4\bar{\rho}_2z^2\bar{z}].
 \end{aligned}$$

Comparing the coefficients of the above equation with those in (38), we have

$$\begin{aligned}
 g_{20} &= 2\bar{D}K_1\bar{\rho}_2, & g_{11} &= \bar{D}K_2\bar{\rho}_2, \\
 g_{02} &= 2\bar{D}K_3\bar{\rho}_2, & g_{21} &= 2\bar{D}K_4\bar{\rho}_2.
 \end{aligned} \tag{43}$$

We still need to compute $W_{20}(\theta)$ and $W_{11}(\theta)$ for $\theta \in [-\tau_0, 0)$ for expression of g_{21} . Indeed, we have

$$\begin{aligned}
 H(z, \bar{z}, \theta) &= -2 \operatorname{Re}\{\bar{q}^{*T}(0)f_0(z, \bar{z})q(\theta)\} = -2 \operatorname{Re}\{g(z, \bar{z})q(\theta)\} \\
 &= -g(z, \bar{z})q(\theta) - \bar{g}(z, \bar{z})\bar{q}(\theta) \\
 &= -\left(\frac{g_{20}}{2} \frac{z^2}{2} + g_{11}z\bar{z} + g_{02} \frac{\bar{z}^2}{2} + g_{21} \frac{z^2\bar{z}}{2} + \dots\right)q(\theta) \\
 &\quad - \left(\frac{\bar{g}_{20}}{2} \frac{z^2}{2} + \bar{g}_{11}z\bar{z} + \bar{g}_{02} \frac{\bar{z}^2}{2} + \bar{g}_{21} \frac{z^2\bar{z}}{2} + \dots\right)\bar{q}(\theta).
 \end{aligned}$$

Comparing the coefficients of the above equation with those in (40), it is clear that

$$\begin{aligned}
 H_{20}(\theta) &= -g_{20}q(\theta) - \bar{g}_{02}\bar{q}(\theta), \\
 H_{11}(\theta) &= -g_{11}q(\theta) - \bar{g}_{11}\bar{q}(\theta).
 \end{aligned}$$

It follows from (25) and (42) that

$$\begin{aligned}
 \dot{W}_{20}(\theta) &= AW_{20}(\theta) = i2\omega_0W_{20}(\theta) - H_{20}(\theta) \\
 &= i2\omega_0W_{20}(\theta) + g_{20}q(\theta) + \bar{g}_{02}\bar{q}(\theta) \\
 &= i2\omega_0W_{20}(\theta) + g_{20}q(0)e^{i\omega_0\theta} + \bar{g}_{02}\bar{q}(0)e^{-i\omega_0\theta}.
 \end{aligned}$$

Solving for $W_{20}(\theta)$, we can obtain

$$W_{20}(\theta) = \frac{ig_{20}}{\omega_0}q(0)e^{i\omega_0\theta} + \frac{i\bar{g}_{02}}{3\omega_0}\bar{q}(0)e^{-i\omega_0\theta} + E_1e^{2i\omega_0\theta}. \quad (44)$$

By a similar way, we get

$$W_{11}(\theta) = -\frac{ig_{11}}{\omega_0}q(0)e^{i\omega_0\theta} + \frac{i\bar{g}_{02}}{3\omega_0}\bar{q}(0)e^{-i\omega_0\theta} + E_2,$$

where E_1, E_2 are both two dimensional vectors and can be determined by setting $\theta = 0$ in $H(z, \bar{z}, \theta)$. In fact, we have

$$\begin{aligned} H(z, \bar{z}, 0) &= -2 \operatorname{Re}\{\bar{q}^{*\Gamma}(0)f_0(z, \bar{z})q(\theta) + f_0(z, \bar{z})\} \\ &= -\left(g_{20}\frac{z^2}{2} + g_{11}z\bar{z} + g_{02}\frac{\bar{z}^2}{2} + g_{21}\frac{z^2\bar{z}}{2} + \dots\right)q(\theta) \\ &\quad -\left(\bar{g}_{20}\frac{z^2}{2} + \bar{g}_{11}z\bar{z} + \bar{g}_{02}\frac{\bar{z}^2}{2} + \bar{g}_{21}\frac{z^2\bar{z}}{2} + \dots\right)\bar{q}(\theta) \\ &\quad + \begin{pmatrix} K_1z^2 + K_2z\bar{z} + K_3\bar{z}^2 + K_4z^2\bar{z} \\ 0 \end{pmatrix}. \end{aligned}$$

Comparing the coefficients of the above equation with those in (40), it follows that

$$\begin{aligned} H_{20}(0) &= -g_{20}q(0) - \bar{g}_{02}\bar{q}(0) + \begin{pmatrix} K_1 \\ 0 \end{pmatrix}, \\ H_{11}(0) &= -g_{11}q(0) - \bar{g}_{11}\bar{q}(0) + \begin{pmatrix} K_2 \\ 0 \end{pmatrix}. \end{aligned} \quad (45)$$

By the definition of A and equations (25), (42), we can get

$$\begin{aligned} \int_{-\tau_0}^0 d\eta(\theta)W_{20}(\theta) &= AW_{20}(0) = i2\omega_0W_{20}(0) - H_{20}(0), \\ \int_{-\tau_0}^0 d\eta(\theta)W_{11}(\theta) &= AW_{11}(0) = -H_{11}(0). \end{aligned}$$

Notice that

$$\left(i\omega_0I - \int_{-\tau_0}^0 e^{i\omega_0\theta} d\eta(\theta)\right)q(0) = 0, \quad \left(-i\omega_0I - \int_{-\tau_0}^0 e^{-i\omega_0\theta} d\eta(\theta)\right)\bar{q}(0) = 0.$$

Thus, we can obtain

$$\left(2i\omega_0I - \int_{-\tau_0}^0 e^{2i\omega_0\theta} d\eta(\theta)\right)E_1 = \begin{pmatrix} K_1 \\ 0 \end{pmatrix}.$$

Similarly, we have

$$\left(\int_{-\tau_0}^0 d\eta(\theta) \right) E_2 = - \begin{pmatrix} K_2 \\ 0 \end{pmatrix},$$

where $E_1 = (E_1^{(1)}, E_1^{(2)})^T$, $E_2 = (E_2^{(1)}, E_2^{(2)})^T$.

Hence, it follows that

$$\begin{pmatrix} i2\omega_0 - a & -b \\ -ce^{-2i\omega_0\tau_0} & i2\omega_0 - de^{-2i\omega_0\tau_0} \end{pmatrix} \begin{pmatrix} E_1^{(1)} \\ E_1^{(2)} \end{pmatrix} = \begin{pmatrix} K_1 \\ 0 \end{pmatrix} \tag{46}$$

and

$$\begin{pmatrix} a & b \\ c & d \end{pmatrix} \begin{pmatrix} E_2^{(1)} \\ E_2^{(2)} \end{pmatrix} = - \begin{pmatrix} K_2 \\ 0 \end{pmatrix}. \tag{47}$$

From (46) and (47) we can obtain

$$E_1^{(1)} = \frac{K_1(i2\omega_0 - de^{-2i\omega_0\tau_0})}{-4\omega_0^2 - 2ia\omega_0 - 2id\omega_0e^{-2i\omega_0\tau_0} + (ad - bc)e^{-2i\omega_0\tau_0}},$$

$$E_1^{(2)} = \frac{K_1ce^{-2i\omega_0\tau_0}}{-4\omega_0^2 - 2ia\omega_0 - 2id\omega_0e^{-2i\omega_0\tau_0} + (ad - bc)e^{-2i\omega_0\tau_0}},$$

and

$$E_2^{(1)} = \frac{-K_2d}{ad - bc}, \quad E_2^{(2)} = \frac{K_2c}{ad - bc}.$$

Based on the above analysis, we can see that each g_{ij} in (43) is determined by parameters and delays in (5). Thus, we can compute the following quantities:

$$C_1(0) = \frac{i}{2\omega_0} \left(g_{20}g_{11} - 2|g_{11}|^2 - \frac{1}{3}|g_{02}|^2 \right) + \frac{g_{21}}{2},$$

$$\mu_2 = -\frac{\text{Re}\{C_1(0)\}}{\text{Re}\lambda'(0)}, \quad \beta_2 = 2 \text{Re}\{C_1(0)\}, \tag{48}$$

$$T_2 = -\frac{\text{Im}\{C_1(0)\} + \mu_2 \text{Im}\lambda'(0)}{\omega_0},$$

which determine the quantities of bifurcation period solutions in the center manifold at the critical values τ_0 .

By the result of Hassard et al. [15], we have the following theorem.

Theorem 2. *In (48), the following results hold:*

- (i) *The sign of μ_2 determines the directions of the Hopf bifurcation: if $\mu_2 > 0$ ($\mu_2 < 0$), then the Hopf bifurcation is supercritical (subcritical).*
- (ii) *The sign of β_2 determines the stability of the bifurcating periodic solutions: the bifurcating periodic solutions are stable (unstable) if $\beta_2 < 0$ ($\beta_2 > 0$).*
- (iii) *The sign of T_2 determines the period of the bifurcating periodic solutions: the period increase (decreases) if $T_2 > 0$ ($T_2 < 0$).*

5 Numerical simulations

In this section, we use the formulas obtained in Sections 3 and 4 to verify the existence of the Hopf bifurcation and calculate the Hopf bifurcation value and the direction of the Hopf bifurcation of system (5) with $p = 0.2, \tau_R = 1, \tau_{\min} = 0.3, T_0 = 2$.

By (6) and (7), we can obtain $r^* = 2.2942, B^* = 1.8353, a = -0.8075, b = 0.1376, c = 0.4, d = -0.5$. Based on (15) and (16), we have $\omega_0 = 0.4488, \tau_0 = 3.6435$. These calculations show that the system equilibrium (r^*, B^*) is asymptotically stable when $\tau < \tau_0$ (see Figs. 1–3, $\tau = 3.6 < \tau_0 = 3.6435$).

When τ passes through the critical value $\tau_0 = 3.6435, (r^*, B^*)$ loses its stability and a Hopf bifurcation occurs, i.e., a family of periodic solution bifurcates out from (r^*, B^*) as shown in Figs. 4–6. From Theorem 2 the bifurcation periodic solutions are unstable since $\beta_2 = 0.0021 > 0$, the Hopf bifurcation is subcritical since $\mu_2 = -0.0194 < 0$. Since $T_2 = -0.0243 < 0$, the period of the bifurcating periodic solutions decrease as τ decreases.

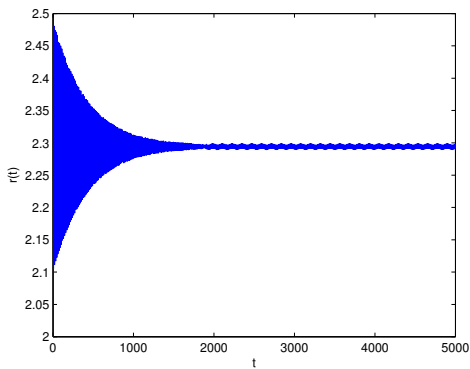


Figure 1. Waveform plot of $t-r(t)$ with $\tau = 3.6$.

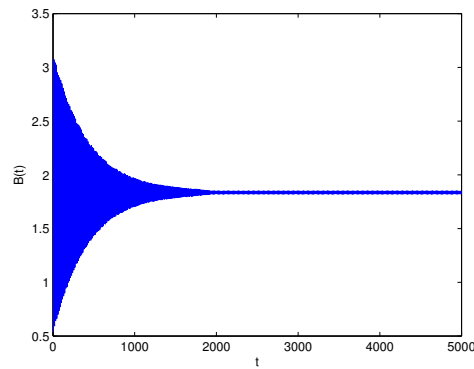


Figure 2. Waveform plot of $t-\hat{B}(t)$ with $\tau = 3.6$.

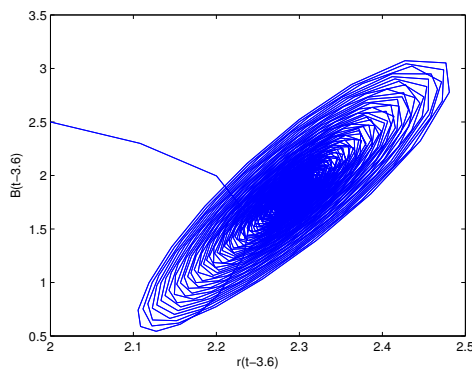


Figure 3. Phase plot of $r(t - 3.6) - \hat{B}(t)$ with $\tau = 3.6$.

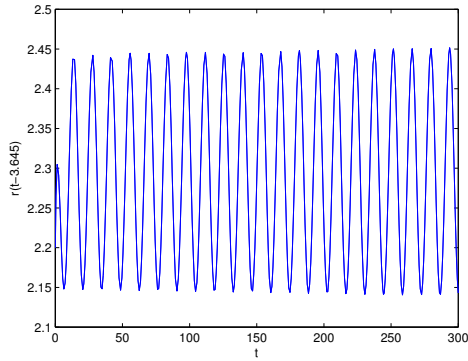


Figure 4. Waveform plot of $t-r(t)$ with $\tau = 3.645$.

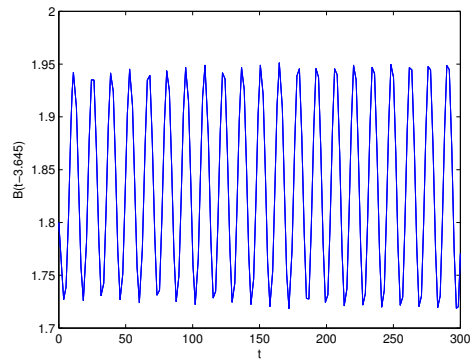


Figure 5. Waveform plot of $t-\widehat{B}(t)$ with $\tau = 3.645$.

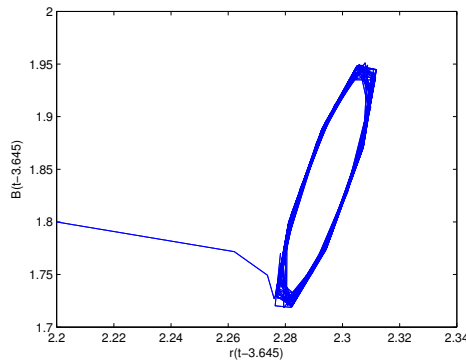


Figure 6. Phase plot of $r(t-3.645) - \widehat{B}(t-3.645)$ with $\tau = 3.645$.

6 Conclusions

In this paper, we first model a Westwood+ TCP with communication delay in mobile cloud computing networks. By analyzing the distribution of the roots of the corresponding characteristic equation, we have obtained some sufficient conditions for the stability of Westwood+ TCP with communication delay. Using communication delay as the bifurcation parameter, we have shown that a Hopf bifurcation occurs when this parameter passes through a critical value, i.e., a family of periodic orbits bifurcates from the equilibrium. The direction of Hopf bifurcation and the stability of the bifurcating periodic orbits are also discussed by using the center manifold theorem and the normal form theory. Simulation results have verified and demonstrated the correctness of the theoretical results.

References

1. S. Athuraliya, V.H. Li, S.H. Low, Q. Yin, REM: Active queue management, *IEEE Network*, **15**(3):48–53, 2001.

2. C. Barakat, E. Altman, Bandwidth tradeoff between TCP and link-level FEC, *Comput. Netw.*, **39**:133–150, 2002.
3. K. Cooke, Z. Grossman, Discrete delay, distributed delay and stability switches, *J. Math. Anal. Appl.*, **86**:592–627, 1982.
4. D. Ding, J. Zhu, X. Luo, Hopf bifurcation analysis in a fluid flow model of internet congestion, *Nonlinear Anal., Real World Appl.*, **10**:824–839, 2009.
5. D. Ding, J. Zhu, X. Luo, Y. Liu, Delay induced hopf bifurcation in a dual model of Internet congestion control algorithm, *Nonlinear Anal., Real World Appl.*, **10**:2873–2883, 2009.
6. T. Dong, X. Liao, T. Huang, Dynamics of a congestion control model in a wireless access network, *Nonlinear Anal., Real World Appl.*, **14**:671–683, 2013.
7. S. Floyd, V. Jacobson, Random early detection gateways for congestion avoidance, *IEEE/ACM Transactions on Networking*, **1**(4):397–413, 1993.
8. L.A. Grieco, S. Mascolo, Performance evaluation and comparison of Westwood+, New Reno, and Vegas TCP congestion control, *ACM SIGCOMM Computer Communication Review*, **34**:25–38, 2004.
9. L.A. Grieco, S. Mascolo, Mathematical analysis of westwood+ tcp congestion control, *IEE Proc., Control Theory Appl.*, **152**(1):35–42, 2005.
10. S. Guo, S. Deng, D. Liu, Hopf and resonant double hopf bifurcation in congestion control algorithm with heterogeneous delays, *Nonlinear Dyn.*, **61**:553–567, 2010.
11. S. Guo, X. Liao, C. Li, Stability and Hopf bifurcation analysis in a novel congestion control model with communication delay, *Nonlinear Anal., Real World Appl.*, **9**:1292–1309, 2008.
12. S. Guo, X. Liao, Q. Liu, C. Li, Necessary and sufficient conditions for hopf bifurcation in an exponential RED algorithm with communication delay, *Nonlinear Anal., Real World Appl.*, **9**(4):1768–1793, 2008.
13. S. Guo, X. Liao, Q. Liu, H. Wu, Linear stability and hopf bifurcation analysis for exponential RED algorithm with heterogeneous delays, *Nonlinear Anal., Real World Appl.*, **10**:2225–2245, 2009.
14. S. Guo, H. Zheng, Q. Liu, Hopf bifurcation analysis for congestion control with heterogeneous delays, *Nonlinear Anal., Real World Appl.*, **11**:3077–3090, 2010.
15. B.D. Hassard, N.D. Kazarinoff, Y.-H. Wan, *Theory and Applications of Hopf Bifurcation*, Cambridge Univ. Press, Cambridge, 1981.
16. V. Jacobson, Congestion avoid and control, *ACM SIGCOMM Computer Communication Review*, **18**(4):314–329, 1988.
17. R. Johari, D.K.H. Tan, End-to-end congestion control for the Internet: Delays and stability, *IEEE/ACM Transactions on Networking*, **9**(6):818–832, 2001.
18. F. Kelly, Mathematical modeling of the internet, in J.M. Ball, J.C.R. Hunt (Eds.), *Proceedings of the Fourth International Congress on Industrial and Applied Mathematics, Edinburg, 5–9 July 1999*, Oxford Univ. Press, Oxford, 1999, pp. 105–116.
19. F.P. Kelly, Fairness and stability of end-to-end congestion control, *Eur. J. Control*, **9**:149–165, 2003.
20. F. Liu, Z.-H. Guan, H.O. Wang, Stability and Hopf bifurcation analysis in a TCP fluid model, *Nonlinear Anal., Real World Appl.*, **12**:353–363, 2011.

21. F. Liu, H.O. Wang, Z.-H. Guan, Hopf bifurcation control in XCP for the Internet congestion control system, *Nonlinear Anal., Real World Appl.*, **13**:1466–1479, 2012.
22. S. Liu, T. Basar, R. Srikant, Exponential-RED: A stabilizing AQM scheme for low- and high-speed TCP protocols, *IEEE/ACM Transactions on Networking*, **13**(5):1068–1081, 2005.
23. S. Mascolo, C. Casetti et al., TCP Westwood: End-to-end bandwidth estimation of efficient transport over wired and wireless networks, in *Proceedings of the Seventh Annual International Conference on Mobile Computing and Networking, July 16–21, 2001, Rome, Italy*, ACM, 2001, pp. 287–297.
24. L. Massoulié, Stability of distributed congestion control with heterogeneous feedback delays, *IEEE Trans. Autom. Control*, **47**(6):895–902, 2002.
25. L. PEI, X. Mu, R. Wang, J. Yang, Dynamics of the Internet TCP-RED congestion control system, *Nonlinear Anal., Real World. Appl.*, **12**:947–955, 2011.
26. G. Raina, Local bifurcation analysis for some dual congestion control algorithms, *IEEE Trans. Autom. Control*, **50**(8):1135–1146, 2005.
27. G. Raina, O. Heckmann, TCP: Local stability and Hopf bifurcation, *Perform. Eval.*, **63**(3):266–275, 2007.
28. B. Rezaie, M.R. Jahed Motlagh, S. Khorsandi, M. Analoui, Hopf bifurcation analysis on an Internet congestion control system of arbitrary dimension with communication delay, *Nonlinear Anal., Real World. Appl.*, **11**:3842–3857, 2010.
29. Z. Wang, T. Chu, Delay induced hopf bifurcation in a simplified network congestion control model, *Chaos Solitons Fractals*, **28**(1):161–172, 2006.
30. M. Xiao, J. Cao, Delayed feedback-based bifurcation control in an internet congestion model, *J. Math. Anal. Appl.*, **332**(2):1010–1027, 2007.
31. M. Xiao, W.X. Zheng, J. Cao, Bifurcation control of a congestion control model via state feedback, *Int. J. Bifurcation Chaos Appl. Sci. Eng.*, **23**(6), Article ID 1330018, 31 pp., 2013.
32. W. Xu, J. Cao, M. Xiao, Bifurcation analysis and control in exponential RED algorithm, *Neurocomputing*, **129**:232–245, 2014.
33. H. Yang, Y. Tian, Hopf bifurcation in REM algorithm with communication delay, *Chaos Solitons Fractals*, **25**(5):1093–1105, 2005.